Rev. Roum. Sci. Techn.– Électrotechn. et Énerg.
Vol. **62**, *4*, pp. 365–370, Bucarest, 2017

DIRECT *S*-POWER CONTROL FOR A DOUBLY FED INDUCTION GENERATOR

NAÏMA MEKKAOUI, MOHAMED-SAÏD NAÏT-SAÏD

Keywords: Doubly fed induction generator (DFIG), Direct *S*-power control (DSPC), Proportional integral (PI) controller, Parameters variation, Imaginary space vector modulation (ISVM), Saturation effect.

This paper deal with an efficient and simple algorithm so-called direct S-power control (DSPC) for a doubly fed induction generator (DFIG) driven through its rotor inverter supplied by the imaginary space vector modulation (ISVM) strategy. The used machine is considered with and without taking account the saturation effect. The DFIG control is done from the calculated rotor voltage related directly to the active and reactive powers injected on the grid network. Both mentioned powers, summarized into apparent power, are treated by the complex formulation simplifying the time of control application. Furthermore, ISVM technique is used without more time computing to generate the mandatory switching pulses within the fixed switching frequency of the supplying rotor inverter. Simulation results obtained from 4 kW DFIG drive system does provide the effectiveness for the injected pure active power into the grid and the robustness against the rotor speed variation.

1. INTRODUCTION

The wind energy systems using doubly fed induction machine (DFIG) have advantages due to variable speed operation and four quadrants active and reactive power capabilities compared with fixed speed induction generator [1, 2]. The stator of DFIG is connected directly to the grid and the rotor is fed by a variable ac voltage source which can be controlled in frequencies according to variable speed of the rotor shaft due to the variation of speed wind, this one is linked to the grid through a bi-directional converter. The rotor inverter allows controlling the produced DFIG active and reactive power to the stator ac supply. It is well known that the field oriented control (FOC) and direct torque control (DTC) are more used than other schemes [3, 4].

DTC schemes are based on a direct control of the torque and the flux magnitudes and has been initiated by Takahashi and Noguchi for low and medium power applications [5]. DTC technique version introduced by Depenbrock for high power application are more popular in industry because it has a simple control scheme whereas assuming less parameter sensitivity and less computational requirements compared with field oriented control (FOC) schemes which also require the current controllers and the coordinate transformations [1, 6, 7]. In the control of the electrical generation, the direct power control (DPC) originated from DTC for induction machines. Several researchers have focused their efforts to progress the DPC techniques that operate at a variable switching frequency [4, 7]. Expensive and complicated ac harmonic filters and power converters, were the consequence of using the variable frequency switching. Recently, to resolve this problem the DPC at a constant switching frequency have been developed for the DFIG [8, 9]. In this work, the developed DPC approach is formatted in complex form allowing to reduce sufficiently the computing time of the control. Thereafter, it is called the direct apparent power control or direct S-power control, abbreviate DSPC. In order to improve the accuracy and to ensure a good performance of this approach, this one should include the saturation in the main flux path, modeled by adjusting the magnetizing inductance as a function of the magnetizing current.

In this paper, active and reactive power controllers and the so-called imaginary space-vector modulation (ISVM) are combined to replace hysteresis controllers used in the proposed DSPC-DFIG drives. With the use of ISVM technique we benefit of both advantages such as lower computing time for its numerical implementation and for its fixed commutation frequency of the inverter. From there, it results a fixed switching frequency of the power converter by employing a simple and smooth algorithm which reduces the harmonics content.

Section 1 has been reserved to the introduction. Section 2 presents the model of doubly fed induction generator in the separate reference frames and afterwards introduces the developed DSPC strategy for the DFIG. Section 3 gives a brief introduction of the ISVM algorithm computing the switching times using the concept of the imaginary switching time [10]. Section 4 presents the accuracy of the simulation results improved by including the saturation to the proposed technique behavior. Section 5 summarizes the conclusion of the present work.

2. DIRECT *S*-POWER CONTROL APPROACH FOR DFIG

Next it will be presented the development of this approach based on complex form calculation of each characterized DFIG variables and form, which the so-called S-power may be transferred to the network grid.

2.1. DFIG-PARK MODEL

The following equations give this model expressed in main rotating synchronous reference frame linked to stator frequency from the wound rotor of the induction machine whereas each complex variable is scripted as $\bar{x} = \bar{x}_d + \mathrm{j}\bar{x}_q$ with $\bar{x}$ may be voltage ($\bar{u}$), current ($\bar{i}$) or flux ($\bar{\Phi}$). The subscripts "d" and "q" indicate the orthogonal Park indices. The indices "*s*" or "*r*" of variable $\bar{x}_{s/r}$ used below are respectively related to the stator and the rotor armatures of the machine [11, 12]:

– *Voltage equations*,

$$\bar{u}_s = R_s\bar{i}_s + \frac{\mathrm{d}\bar{\Phi}_s}{\mathrm{d}t} + \mathrm{j}\omega_s\bar{\Phi}_s \tag{1}$$

Université de Batna, Department of Electrical Engineeirng, Batna 2 University, Avenue Chahid Mohamed Boukhlouf – 05000 – Batna, Algeria; E-mails: mekkaoui_ns@yahoo.fr; medsaidnaitsaid@yahoo.fr

$$\bar{u}_r = R_r \bar{i}_r + \frac{\mathrm{d}\bar{\Phi}_r}{\mathrm{d}t} + \mathrm{j}\omega_r \bar{\Phi}_r \,. \tag{1}$$

– *Flux equations*,

$$\begin{aligned} \bar{\Phi}_s &= L_s \bar{i}_s + M \bar{i}_r \,, \\ \bar{\Phi}_r &= L_r \bar{i}_r + M \bar{i}_s \,, \end{aligned} \tag{2}$$

where: ω_s and ω_r are respectively the stator and rotor frequencies related to speed rotor Ω by

$$\omega_s = \omega_r \pm N_p \Omega \,. \tag{3}$$

The appeared parameters are defined in equations (1)–(3) as follows. R_s, R_r are the resistances and L_s, L_r are the self inductances of the stator and the rotor windings, respectively. *M* is the magnetizing inductance and N_p is the pair poles number.

In order to obtain more accurate results, the saturation effect can be included in the generator model when needed, if the magnetic saturation has the effects on machine it will limit the transient over-shoot current and power on step response of the DPC control [13]. The saturation effect can be achieved by varying mutual inductance as a function of the magnetic current magnitude extracted from typical saturation curve.

2.2. ROTOR FLUX *S*-POWER ESTIMATION

The so-called *S*-power, named apparent stator power, is given in complex from $\bar{S}$ as follows

$$\bar{S} = \bar{u}_s \cdot \bar{i}_s^{\,c} = P + \mathrm{j}Q \,, \tag{4}$$

where *P* and *Q* indicate respectively the stator active and reactive powers and notation $(.)^c$ signifies the complex conjugate.

We consider that the powerful grid imposes the magnitude and frequency of the DFIG stator voltage. The power losses may be neglected and also the derivative stator flux may be assumed zero, by this imposing a steady state sinusoidal regime, as $\mathrm{d}/\mathrm{d}t = 0$. From equations (1) and (4), we can write:

$$\bar{S} = \bar{u}_s \bar{i}_s^{\,c} \approx \mathrm{j}\omega_s \bar{\Phi}_s \bar{i}_s^{\,c}. \tag{5}$$

From equations (2), the stator current can be expressed by the stator and rotor fluxes as follows:

$$\bar{i}_s = (\sigma L_s)^{-1} \bar{\Phi}_s + (\sigma - 1) \cdot (\sigma M)^{-1} \bar{\Phi}_r \quad , \tag{6}$$

where, $\sigma = 1 - M^2 / L_s L_r$ is the factor flux leakage.

Using equations (5) and (6) and adopting that $\bar{u}_s = |\bar{u}_s|$ given by the orientation of the stator voltage vector on d-axis so that $u_{sq} = 0$, therefore we can write $|\bar{\Phi}_s| \approx |\bar{u}_s| / \omega_s$ and the *S*-power from rotor flux may be written as the following expression

$$\bar{S} = B \cdot \bar{\Phi}_r^c + \mathrm{j}A \,, \tag{7}$$

where the constant parameters *A* and *B*, defining the complex relationship between *S*-power and rotor flux, are given as follows

$$A = \frac{1}{\sigma L_s \omega_s} |\bar{u}_s|^2 \text{ and } B = \frac{\sigma - 1}{\sigma M} |\bar{u}_s| \,. \tag{8}$$

From equations (7) and (8), the rotor flux can be directly estimated from *S*-power, which is invariant by usual Park transformation, from the voltage and current measurements of the DFIG in the stationary reference frame through Concordia transformation. Once the conjugate complex rotor flux is estimated, its modulus and phase may be easily obtained.

2.3. DIRECT *S*-POWER CONTROL

Assuming that the core rotor power losses are also neglected, the rotor voltage of the equations (1) allow to write the transfer function as a simple integrator as follows

$$\frac{\bar{\Phi}_r}{\bar{U}_r} = \frac{1}{p} \,, \tag{9}$$

where $p = \dfrac{\mathrm{d}}{\mathrm{d}t}$ is the derivative operator and $\bar{U}_r = \bar{u}_r - \mathrm{j}\omega_r \bar{\Phi}_r$ is the new applied voltage which it is obtained when $\mathrm{j}\omega_r \bar{\Phi}_r$ term may be externally compensated from the *S*-power measurement given by equation (7). On the other hand, this last equation yields as well to establish that the *S*-power varies proportionally with the conjugate rotor flux characterized by the proportional gain *B* given in (8). In this way, referring to equations (7) and (9) the *S*-power may be controlled by the new input rotor voltage $\bar{U}_r$ such formulated in complex form and from that, the feedback control may be written rigorously by the following equations:

$$\frac{\bar{\Phi}_r}{\bar{U}_r} = \frac{1}{p} \Rightarrow \frac{\bar{S}}{\bar{\Phi}_r} \cdot \frac{\bar{\Phi}_r}{\bar{U}_r} = \frac{B}{p} \,, \tag{10}$$

$$\bar{U}_r = \mathrm{PI} \cdot \left(\bar{S}_{ref} - \bar{S} \right), \tag{11}$$

where PI is the proportional and integral controller expressed by $\mathrm{PI} = k_p + \dfrac{k_i}{p}$ with k_p and k_i define its proportional and integral gains. Then the real input rotor voltage $\bar{u}_r$ controlling the DFIG by the direct *S*-power control approach law is then given as:

$$\bar{u}_r = \mathrm{PI} \cdot \left(\bar{S}_{ref} - \bar{S} \right) + \mathrm{j}\omega_r \bar{\Phi}_r. \tag{12}$$

The closed loop *S*-power control is then formulated as transfer function of second order given below, the choice of damping factor ξ and natural frequency ω_n determine adequately the PI gain parameters

$$\frac{\bar{S}^c}{\bar{S}_{ref}^c} = \frac{1 + 2\xi \dfrac{\omega_n}{p}}{1 + 2\xi \dfrac{\omega_n}{p} + \dfrac{\omega_n^2}{p^2}} \,, \tag{13}$$

where

$$\frac{1}{B k_i} = \omega_n^2 \tag{14}$$

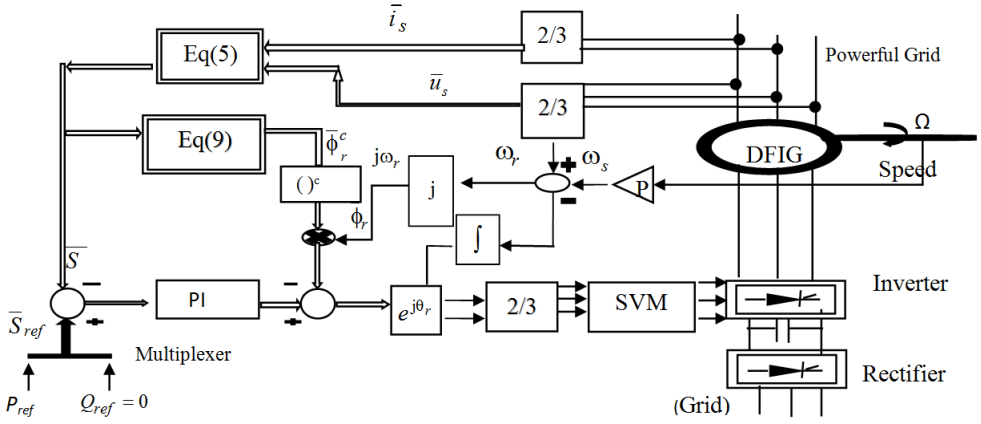

Fig. 1 – Block diagram of DSPC for DFIG.

The block diagram of the direct *S*-power control for the DFIG machine supplying the powerful gird can be illustrated as follows in Fig. 1, to realize an optimal active power transfer to the grid. The reference input is done as pure real number like $\bar{S}_{ref} = P_{ref} + \mathrm{j}0$.

3. IMAGINARY SPACE VECTOR MODULATION (ISVM)

The so-called imaginary space vector (ISVM) control strategy is a novel idea to control the converter. The space vector modulation (SVM) was first presented by a group of German researched in the second half of the 1980's [5, 6]. Since then, a lot of work has been done on the theory and implementation of SVM techniques. SVM compared to conventional sinusoidal PWM method has the following advantages: increasing the voltage utilization rate by 15.47 %, having a lower switching frequency, easier to implement for microprocessor due to simple vector mode switching [10].

In the SVM scheme, the voltage reference vector $\bar{V}_{ref}$ has been approximated by the time averaging over a sampling interval of the two adjacent active voltage vectors ($\bar{V}_1, \bar{V}_2$) and two zero voltage vectors $\bar{V}_{0/7}$. The switching turn-on times, of the two active states and two zero states are utilized to determine the duty cycle information to program the active switching gate signals. In the linear modulation operating region of inverter, the sum times of the two active states is smaller than the duration of the sub cycle. In which, case the remaining time is occupied by using the two zero states. The time segment (T_1, T_2, $T_{0/7}$) of each space vector is determined by the following equations. Figure 2 shows how to compute the times of the applied stator voltage of the conventional SVM for the inverter given from the reference stator voltage calculated by the control scheme according to each six sectors.

$$\bar{V}_{ref} = \left(\frac{T_1}{T_s} \times \bar{V}_1\right) + \left(\frac{T_2}{T_s} \times \bar{V}_2\right) + \left(\frac{T_{0/7}}{T_s} \times \bar{V}_{0/7}\right). \qquad (15)$$

We have, $|\bar{V}_1| = |\bar{V}_2| = \frac{2}{3} V_{dc}$ the time interval can be calculated as follows:

$$\begin{cases} T_1 = \dfrac{\sqrt{3}|\bar{V}_{ref}|}{V_{dc}} T_s \cdot \sin\left(\dfrac{\pi}{3} - \alpha\right) \\ T_2 = \dfrac{\sqrt{3}|\bar{V}_{ref}|}{V_{dc}} T_s \cdot \sin(\alpha) \end{cases}, \qquad (16)$$

$$T_{0/7} = T_s - T_1 - T_2 . \qquad (17)$$

Here, T_s is the sampling time, T_1, T_2 and T_0 are the duration for which V_1 , V_2 and V_0 or V_7 are applied, α is the angle of the applied reference voltage V_{ref} on the stationnary refrence frame and V_{dc} is the dc link voltage.

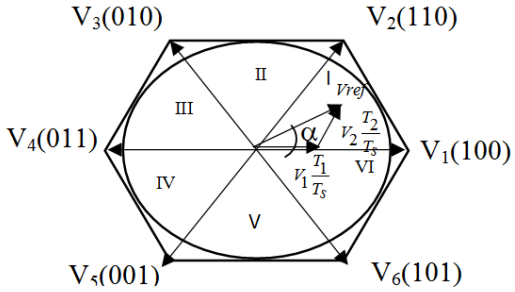

Fig. 2 – Illustration of the computing conventional SVM times.

The conventional SVM above gives a good performance, but the complexity involved is more in calculating angle and sector. To reduce this difficulty in SVM, a novel modulation technique named unified voltage modulation or carrier based SVM is described using the concept of effective time from which the so-called imaginary space vector modulation (ISVM) is built. This technique is easily used for all numerical feedback control implementation without more computing time and it presents a strong advantage for the real time feedback control. Indeed, ISVM technique employs only the instantaneous reference phase voltages for the implementation of the SVM without estimation of angle of reference vector. Below, the imaginary switching time periods indicated by T_{ar}, T_{br} and T_{cr} are proportional to the instantaneous values of the reference stator phase voltages mentioned by V_{AN}, V_{BN} and V_{CN} are defined in [7, 14] like follows. V_{dc} and T_s are defined previously as dc link voltage and sampling time, respectively.

$$\begin{cases} T_{ar} = \left(\dfrac{T_s}{V_{dc}}\right)\cdot V_{AN} \\ T_{br} = \left(\dfrac{T_s}{V_{dc}}\right)\cdot V_{BN} \\ T_{cr} = \left(\dfrac{T_s}{V_{dc}}\right)\cdot V_{CN} \end{cases}. \quad (18)$$

When the instantaneous reference voltages are negative, then the corresponding switching times also become negative. Hence, these times are called as imaginary switching times. The corresponding active vector switching times T_1 and T_2, if the reference voltage vector falls in sector-1, may be expressed as follows:

$$\begin{cases} T_1 = T_{ar} - T_{br} \\ T_2 = T_{br} - T_{cr} \end{cases}. \quad (19)$$

For each sampling time, the maximum and minimum values of the imaginary switching times and the so-called effective time may be computed by the following formula:

$$T_{eff} = T_{\max} - T_{\min}. \quad (20)$$

If the imaginary switching times have been calculated from their instantaneous values of the reference phase voltages values according to equation (18), then the maximum and minimum values can be also calculated by using (20). In that case, the effective time during which the induction motor is effectively connected to the source (that is the power will be transferred to the motor from source) is well determined.

To generate the actual switching pattern which preserves the effective time, the zero sequence is subjoined to the phase voltage time. In order to locate the effective time at the center of the sampling time, the zero sequence voltage has to be symmetrically distributed at the beginning and end of one sampling period as shown in Fig. 3 which illustrates the so-called imaginary times SVM.

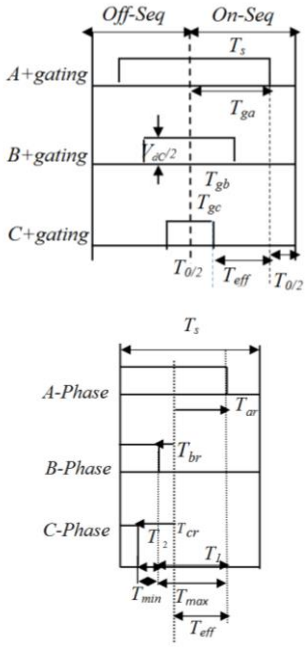

Fig. 3 – Illustration of SVM from imaginary times computing: a) sequence and gating times in sector 1; b) corresponded SVM times determination.

Therefore, a time-shifting operation will be applied to the imaginary switching times to generate the actual gating times (T_{ga}, T_{gb}, T_{gc}) for each inverter arm. This task is accomplished by adding the same value to the imaginary times as follows [15]:

$$\begin{cases} T_{ga} = T_{ar} + T_{offset} \\ T_{gb} = T_{br} + T_{offset} \\ T_{gc} = T_{cr} + T_{offset} \end{cases} \quad (21)$$

$$T_{offset} = \frac{T_0}{2} - T_{min}, \quad (22)$$

T_{offset} is the offset-time.

4. SIMULATION RESULTS AND DISCUSSION

The machine data are given in the Appendix. In order to validate our approach, simulation tests were carried out using the proposed control scheme as illustrated on Fig. 1. The testing conditions, with a horizon simulation time during 3 seconds, are defined such that the imposed variable speed of the shaft rotor changes from 157 rad/s to 160 rad/s while the reactive power is fixed at 0 VAR. During the simulations, the sampling period has been set to 200 μs. The switching frequency of the so-called imaginary SVM technique has been effected at 5 kHz. The simulation results of the proposed SPDC of the DFIG are shown in Figs. 4 and 5.

The imposed rotor speed and the active power reference are mentioned by the notation Ω_{ref} and P_{ref}:

– for $0 \le t \le 0.7$ s, Ω_{reff} =157 rad/s and P_{ref}= 0 W;

– for $0.7 \le t \le 1.2$ s, Ω_{reff} = 158.5 rad/s and P_{ref}= –2 000 W;

– for $1.2 \le t \le 2.5$ s, Ω_{reff} = 160 rad/s and P_{ref} = –4000 W.

The proposed control strategy reveals a fast dynamic response and the active and reactive powers track their desired reference values within few milliseconds without any recorded effect due to speed and the parameters variations. Note that the stator current harmonics are sufficiently reduced by this proposed DSPC scheme as shown in Fig. 4 where THD = 1.8% that may be considered very important for clean and no polluted network.

To reinforce the proposed control strategy of generator model, the simulations have been made including a generator model with and without saturation effect. Both simulations are shown in Fig. 4a.

Rotor flux of saturated model is clearly faster than the unsaturated model in the transient state. So, saturation effect can be incorporated more importantly to improve the transient performances of the SPDC of the DFIG without disturb the steady state regime [13].

Furthermore, the effect of the variation in sampling time is indicated by Fig. 5f. This last demonstrates graphically the response of the generator model for both 5 kHz and 10 kHz when a step change is given to the active power. We notice a better performance of the machine at 5 kHz, in contrast, it has less performance at 10 kHz.

To verify that DFIG parameters variations do not cause a significant effect on the control strategy performance, a simulation with 50% variation in all inductances has been

performed. The results are depicted in Fig. 5, even with such large inductance errors the system response is good enough and the system maintains its high performances under both steady-state and transient regimes. The obtained results demonstrate that the proposed DFIG system control by DSPC scheme, which operates at the variable speed, may be well utilized as an interesting solution in renewable energy area, and furthermore it may be implemented by less computing time.

5. CONCLUSION

This paper presents simulation results of direct *S*-power control method (DSPC) for DFIG drives to control the active and reactive powers directly without the need of the reference frame transformation, neither the current controller. The developed so-called *S*-power direct control law of the DFIG by the complex formulation allows also having an optimized algorithm of the DFIG law control. Furthermore, the imaginary SVM modulation strategy is then used permitting to sufficiently reduce the computation time for its easy numerical implementation. Because the conventional tools like hysteresis comparator and switching look-up table are substituted by this imaginary space-vector modulation (ISVM), the active and reactive powers have been well controlled with a reduced time computing and at fixed switching frequency of the inverter. Extensive simulations confirm the effectiveness and realizing high performance of the proposed method under steady state and transient conditions. The simulations confirm the effectiveness and the robustness of the power controller during several operating conditions and variation of machine parameters. Thus, this DSPC strategy accompanied by ISVM becomes an interesting tool for DFIG feedback control from the point of view of the optimization of the control algorithm and the facility of the numerical implementation.

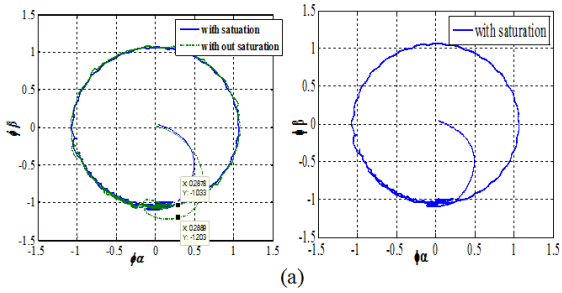

(a)

Fig. 4 – a) Rotor flux trajectory using a model without saturation effects (dotted line) and with saturation effects (solid line) left and right of the figure.

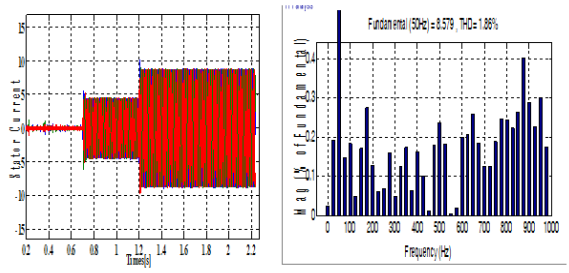

b) c)

Fig. 4 – The proposed direct power control's: b) 3-phases stator currents, c) stator current harmonic spectra phase-A; with nominal all inductance.

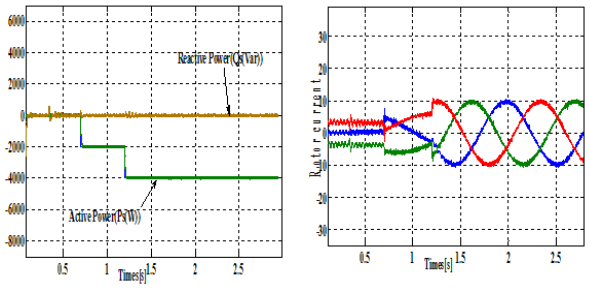

d) f)

Fig. 4 – The proposed direct power control's: d) reactive and active power step; f) 3-phases rotor currents, with nominal all inductance.

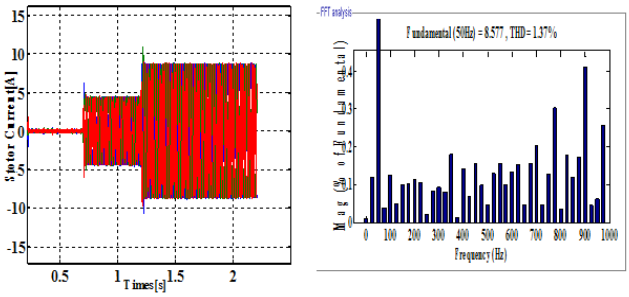

a) b)

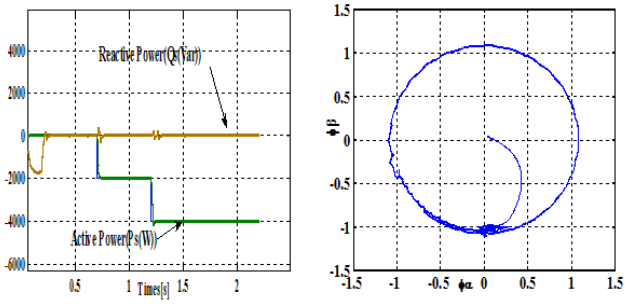

c) d)

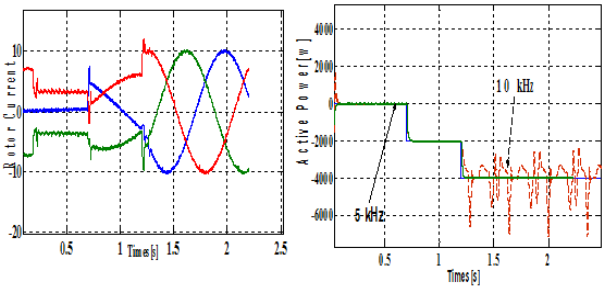

e) f)

Fig. 5 – The proposed direct power control's: a)3-phase stator current; b) stator current harmonic spectra in phase-A; c) active and reactive power step responses; d) trajectory rotor flux; e) 3-phase rotor current; f) active power step responses at 5 kHz and 10 kHz; with 0.5 L_s, 0.5 M, 0.5 L_r.

Received on November 27, 2016

REFERENCES

1. W. Leonhard, *Control of Electrical Drives*, London, U.K., Springer- Verlag, 2001.
2. R.W. De Doncker, S. Muller, M. Deicke, *Doubly fed induction generator systems for wind turbines*, IEEE Ind. Appl. Mag., **8**, *3*, pp. 26–33 (2002).
3. A. Petersson, L. Harnefors, T. Thiringer, *Evaluation of current control methods for wind turbines using doubly-fed induction machines*, IEEE Trans. Power Electron., **20**, *1*, pp. 227–235 (2005).
4. L. Xu, P. Cartwright, *Direct active and reactive power control of DFIG for wind energy generation*, IEEE Trans. Energy Convers., **21**, *3*, pp. 750–758 (2006).
5. Takashi, T. Noguchi, *A new quick-response and high-efficiency control of an induction motor*, IEEE Trans. Industry Applications, **IA-22**, *5*, pp. 820–827 (1986).
6. M. Depenbrock, *Direct self-control (DSC) of inverter-fed induction machine*, IEEE Trans. Power Electron., **PE-3**, *4*, pp. 420–429 (1988).
7. R. Datta, V.T. Ranganathan, *Direct power control of grid-connected wound rotor induction machine without rotor position sensors*, IEEE Trans. Power Electron, **16**, *3*, pp. 390–399 (2001).
8. W.-S. Kim, S.-T. Jou, K.-B. Lee, *Direct power control of a doubly fed induction generator with a fixed switching frequency*, Journal of Power Electronics, **9**, *5*, pp. 781–791 (2009).
9. A.J.S. Filho de Oliveira Filho, E.R. Filho, *Predictive Control Strategy for Doubly – Fed Induction Generator Direct Power Control*, IEEE/1AS International Conference on Industry Application (INDUSCON), 2010.
10. Dae-Woong Chung, Joohn-Sheok Kim, Seung-Ki Sul, *Unified voltage modulation technique for real-time three-phase power conversion*, IEEE Trans. Ind. Applicat., **34**, *2*, pp. 374–380 (1998).
11. J. Lesenne, F. Notelet, G. Séguier, *Introduction à l'électrotechnique approfondie*, Technique et documentation, Paris, 1981.
12. J.P. Louis, *Modèles pour la commande des actionneurs électriques*, Hermès Science Publications, Lavoisier, 2004.
13. L. Wang, J. Jatskevich, *Including Magnetic Saturation in Voltage-Behind-Reactance Induction Machine Model for EMTP-Type Solution*, IEEE Transactions on Power Systems, **25**, *2*, pp. 975–987 (2010).
14. Y. Lei, A. Mullane, G. Lightbody and R. Yacamini, *Modeling of the Wind Turbine with a Doubly Fed Induction Generator for Grid Integration Studies*, IEEE Transactions on Energy Conversion, **21**, *1* (2006).

APPENDIX

The used machine parameters

Parameters	Notation
Resistance of the rotor	2 Ω
Resistance of the stator	1.2 Ω
Inductance of the rotor	0.156 H
Inductance of the stator	0.158 H
Mutual inductance	0.150 H